

Region-based active contour JSEG fusion technique for skin lesion segmentation from dermoscopic images.

Rabia Javed^{1,3*}, Mohd Shafry Mohd Rahim¹, Tanzila Saba², Muhammad Rashid⁴

¹Department of Engineering, Universiti Teknologi Malaysia, Johor Bahru, Malaysia

²College of Computer and Information Sciences, Prince Sultan University, Riyadh, Saudi Arabia

³Department of Computer Science, Lahore College for Women University, Jail Road, Lahore, Pakistan

⁴Department of Computer Science, Comsats University Islamabad (Wah Campus), Wah Cantt, Pakistan

Abstract

Malignant melanoma is one of the most aggressive forms of skin cancer which must be necessary to be diagnosed at the initial stage for effective treatment. Melanoma affects the patient life even it can become a reason of death if its diagnosis is not accomplished on time. Through a rough pigment network and some suspicious signs can be helpful for diagnosis the melanoma from dermoscopic images. According to the clinical studies, for dermatologists, it is quite difficult to identify these signs at the initial stage of melanoma. So, it is important to propose an automated system which can efficiently be identified and differentiate between benign and malignant melanoma. The main focus of this research article is to improve the skin lesion segmentation from low contrast and under/over segmented dermoscopic images through fusing the region based active contour method with JSEG method. The proposed fused segmentation technique gain 95.3% accuracy and through our proposed feature vector the Gaussian classifier achieved the promising results as sensitivity 97.7%, specificity 96.7%, and accuracy 97.5% with handling the special dermoscopic image cases which are comparatively much better than numerous exiting techniques.

Keywords: Melanoma, Region-based, Active contour, Image fusion, Dermoscopic image.

Accepted September 19, 2019

Introduction

Skin cancer is the development of uncontrollable abnormal skin cells. Generally, there are three types of skin cancer: Basal Cell Carcinoma (BCC), Squamous Cell Carcinoma (SCC), and Malignant Melanoma (MM) [1]. Basal, squamous and other types of skin cancer excluding melanoma grouped as Non-Melanoma Skin Cancer (NMSC). Melanoma is less common but more dangerous type as compare to the other two (BCC, SCC). For the reason, that the melanoma spread one part to another part of the body. According to the statistic report of 2018, now in the U.S, the 91,270 (about 55,150 in males and 36,120 in females) estimated cases will be recorded and 9,320 (about 5,990 in males and 3,330 in females) will be estimated the death rate [2]. Here, is right now an extraordinary enthusiasm for the advancement of PC supported determination frameworks that can help the clinical assessment of dermatologists.

Methodology

The standard methodology in programmed dermoscopic image investigation has generally three phases: 1) segmentation, 2)

feature extraction, and 3) classification. For different kind of diseases variety of imaging techniques have been introduced for better and accurate disease detection. For the skin lesion detection, on 1987 dermoscopy or Epiluminescence microscope (ELM) was first depicted [3]. Dermoscopy is a magnified and non-invasive diagnosis procedure for patients. But for accurate detection of melanoma, it all depends on the experience of dermatologists. The dermoscopic dataset contains a variety of images in which image have skin tone variation, and artifacts like hairs, bubbles, ink, and ruler maker, etc., lesion location and the lesion itself have variation in terms of texture, shape, location, and size. So, for robust segmentation algorithm designing for the skin lesion, there should need to cater all of these factors also. Among the many reasons, one of the major challenging tasks which are till then not solved is segment the poor/low contrast dermoscopic images. The differentiating between normal and lesion skin from low contrast images is much harder for dermatologist even computer-aided systems are failed to segment this kind of images. Because of these reasons, it is analyzed that, there should be a fused technique which will deal with these varieties of skin lesion dermoscopic images.

Skin lesion accurate segmentation is very essential toward the detection and classification of melanoma. The essential advantages of using intelligent systems are precise translations for nearly a wide range of signs in the electromagnetic range from gamma to radio waves. Then again, the human eye is constrained to the noticeable light band range as it were. Also, the clinical procedure of melanoma identification is quite difficult. These propelled machine learning strategies not just help specialists for exact discoveries yet additionally catching on quickly and are very nearly taking exact choices. Man-made brainpower is currently getting more knowledge into our lives as choices in a few spots are taken by the machines because of a leap forward in machine learning. This is a reality that specialists are covering diverse genuine spaces while supporting them with cutting-edge machine learning techniques. Lately, most of the segmentation technique is only works well on high contrast skin lesion dermoscopic images and fail in cases of low contrast and under/segmented images. In this article, the crucial focus is to segment the low contrast as well as under/over segmented lesion by fusing the region-based active contour and JSEG techniques. The major contributions are: to deal with under/over segmented images is proposed a region-based active contour method and low contrast skin lesion dermoscopic images handle by implementing JSEG technique. An image fusion technique is also proposed on two segmented images get by apply region-based active contour and JSEG techniques. This study will be useful to assist patient and dermatologists to speed up the process of diagnosis and will be helpful in their practice. This will help save time so more patients can be served.

Related Work

Since the dawn of the digital age, computers have been at the forefront of technological advancements. Due to Moore's law [4], they are becoming efficient ever so more. In recent times artificial intelligence and deep learning have opened up ways to improve many technologies previously thought impossible [5], more importantly in the field of medicine, health, and science [6]. In the field of medicine, the digital image is playing a major part. Many new technologies have proved to be amazing at analyzing images with different aspects of diseases [7,8]. The simplest type of image segmentation is a threshold-based technique. Global thresholding, variable thresholding, and multiple thresholding are three basic types of thresholding Stanley portrayed another segmentation calculation algorithm in view of histogram thresholding and shading space channel for skin injury discovery [9]. Also, Iyatomi proposed a DTEA segmentation calculation algorithm to encourage the high recurrence parts and after that thresholding with Otsu system [10]. Additionally, Stanley presented a different thresholding system for a computerized technique for melanoma determination [9]. Low-level techniques of segmentation do not have the ability to differentiate the objects in an image in contrast semantic segmentation has robot vision and understanding of objects in an image. The semantic

segmentation techniques of processing the image are also followed by different deep learning networks such as convolutional neural network (CNN), fully convolutional networks (FCNs), U-Net, and SegNet, described a semantic segmentation technique using FCN [11,12]. For evaluation of their technique, they use ISIC 2017 and achieved promising results but still, their technique produced some fail cases. These fail cases are shown in the figure where the first row show inaccurate results for the benign and second-row show for melanoma Yuan and Lo [13] described a deep learning method "convolutional deconvolutional neural network (CDNN)" for segmentation of skin lesion of ISIC 2017 dataset. In their method, each layer of convolution and deconvolution used the rectified linear units (ReLU) for activation function. Their method achieves 93% accuracy but still, improvement is needed in the segmentation part, Yu L present a skin segmentation method based on fully convolutional residual network (FCRN) [14]. Their segmentation techniques achieved 94% accuracy but have some failure cases due to the low contrast images. Saliency-Based Segmentation is also used by Rashid works well where the background is complex [15].

Region-based segmentation methods deal with the over-segmentation. Basically, region-based segmentation methods depend on the threshold value and gave efficient segmentation results on the homogenous interest of the region in the image. In different applications, the researcher used this method to overcome this problem. The dermatologist-like tumor extraction algorithm (DTEA) is presented by Iyatomi H that used a region growing method which gave the result near to dermatologist [16]. By combining the region-based active contour and edge-based method takes advantage of both methods [17]. The function or SPF (signed pressure force) define by global means taken from Chan TF which is the most famous region-based method. It deals with constant intensity detail of region so in inhomogeneity [18], it will not perform well segmentation. To solve this problem Li proposed a method based on the local region method which relies on the kernel function [19].

Proposed Architecture

The low contrast and under/over segmented dermoscopic images still gave a challenging task for segmentation. The architecture of the proposed method as shown in Figure 1, are solved the current segmentation issues by tackling all of these dermoscopic images. To overcome the problem of low contrast images, firstly local and global contrast stretching is performed in the pre-processing step. Secondly, the region of interest cannot extract properly in the presence of hair limitation in dermoscopic images. To remove the unwanted hair, DullRazor method is applied [20]. For extraction of the infected region, two segmentation methods is applied with enchantment. Firstly, the region-based active contour method (RBAC) applied for under and over segmented images. After that, J-image segmentation (JSEG) for skin

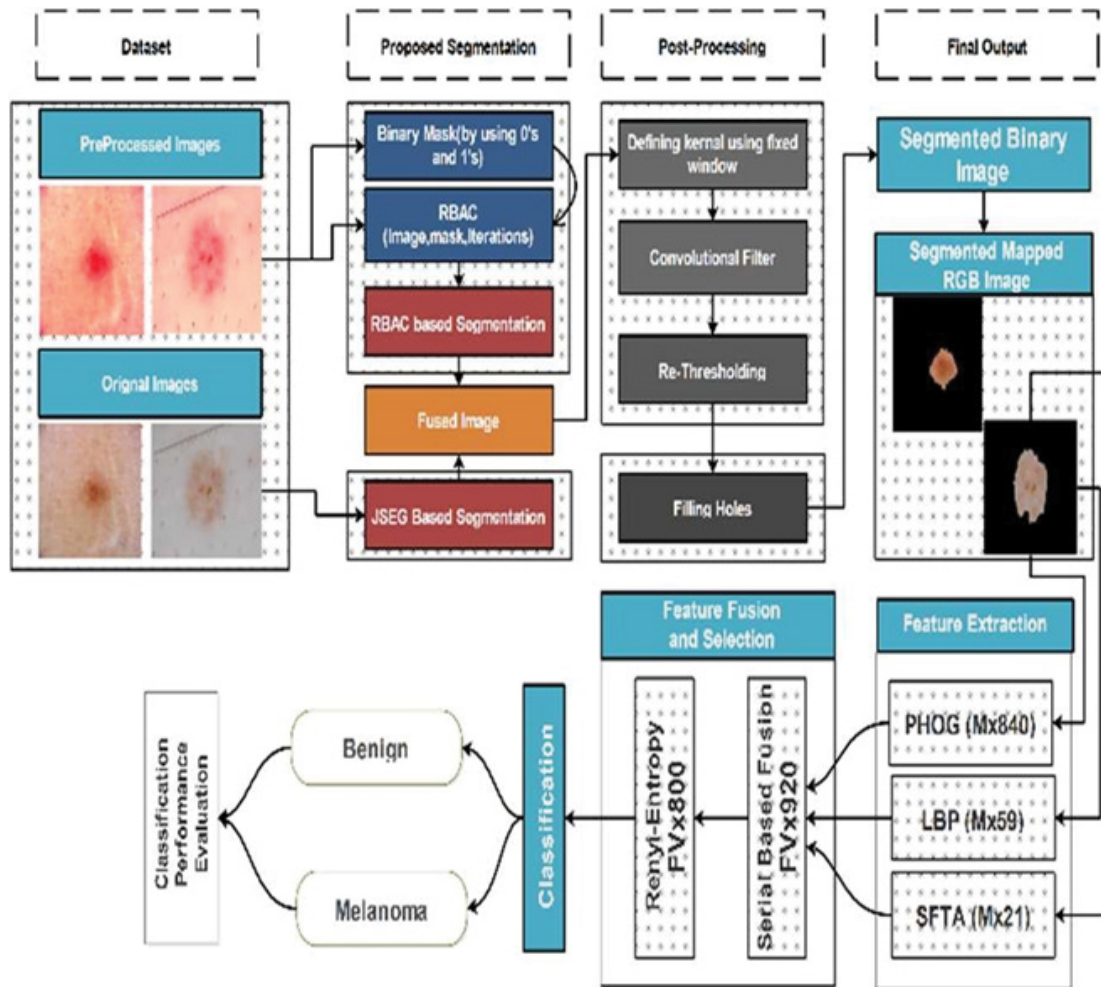


Figure 1. Flow diagram of proposed Architecture.

lesion segmentation is applied and finally, the outputs of both techniques are fused by a fusion imaging technique. RBAC segmentation has many advantages over other segmentation techniques especially for over segmented dermoscopic images it gave good results. The proposed fused segmented technique is specially deal with the low contrast as well as over/under segmented image segmentation problem.

Pre-processing

In pre-processing, the image enhancement is performed on dermoscopic images for high contrast, the better quality of a region of interest (ROI) or enhancing their performance for analyzing and diagnosis process in computer-aided applications (CADs) [21]. To improve the quality of the dermoscopic image local and global contrast stretching technique is used [22] as shown in Figure 2. In this technique, basically, the normalization of the image is changed by defining the range for intensity value [23]. Many different techniques for contrast stretching have been proposed in the previous studies Kaur et al. The DullRazor technique is applied to remove hairs from a skin lesion dermoscopic image [20].

Proposed segmentation model

The contrast stretched image is provided to the RBAC, in which a binary mask is created with a size of the input

image. This mask, contrast stretched image, and the number of iterations for region growing is performed and get the first binary segmented image. The “Region-Based Active Contour Segmentation” is started from a fixed mask. Basically, the purpose of creating the binary mask is to make a difference between background and foreground which is a region of interest in the skin lesion dermoscopic images. Here, the region of interest indicated by the pixel value of 1 and the background presented by the 0-pixel value. After getting the segmented binary image, this binary mask image is mapped into the input image. Then starts wrapping itself around the shape of active contour where it found. It works iteratively, here almost on 500 iterations RBAC gave the much better results of segmentation. The existing region-based active contour method only works on homogeneous (one color) but in low contrast images we need to work on multiple colors so where the method is changed by adding heterogeneity in the method.

Similarly, the input image is passed to JSEG based segmentation; the second binary segmented image is achieved. In J-segmentation technique, there are three basic steps firstly quantization for color space is performed to reduce the same colors from input images. Region merging technique is used in which the same colors merge into one class. Then this binary mask image is mapped into

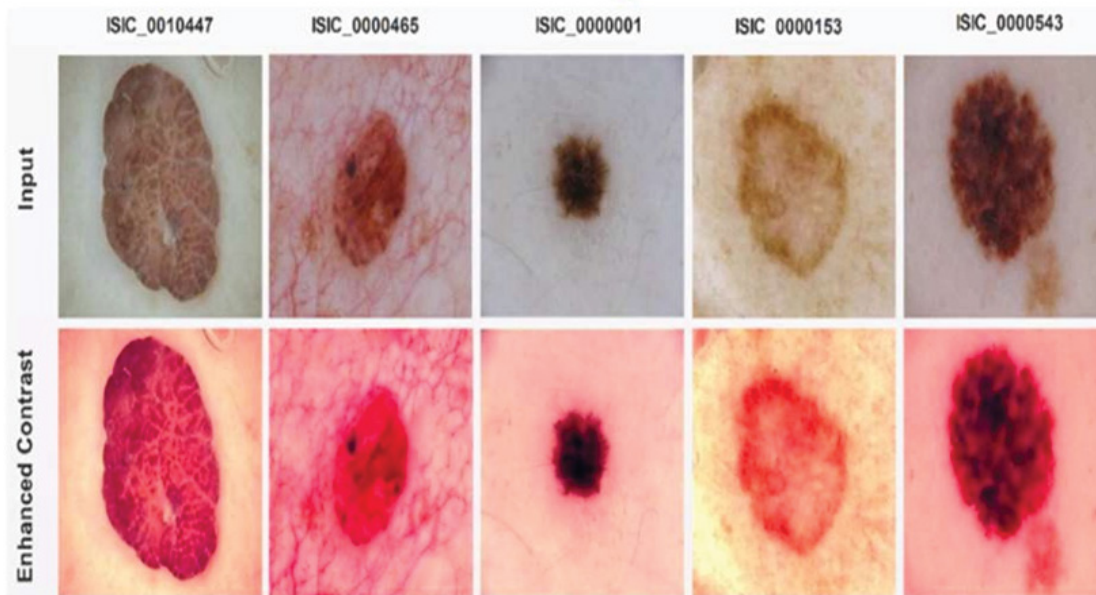


Figure 2. Pre-processing after image enhancement.

the original image. J-value is calculated for the quantized image to placing into the window [24]. To obtain better accuracy for skin lesion segmentation, both binary outputs are fused by applied a spatial domain fusion imaging. In which both segmented images are melted together from different modalities to create a new fused image.

The detail process of the proposed segmentation method is also illustrated in Figure 3.

To explain more clearly mathematical representation is presented below:

$$(c) = \sum O \dot{S} \dot{I} \dot{S} \dot{N} ((a), (b)) \quad (1)$$

Here, in the (1) 'I(c)' represent the proposed fused image which gets after taking the merging the segmented image 'I(a)' and segmented image 'I(b)'. The segmented image 'I(a)' is the output image of the region-based active contour method and the segmented image 'I(b)' is the output image of the JSEG method. Post-processing is applied to the final segmented image which has the sharp edges and notches of the segmented image which is causing less accuracy. To overcome this, take a window size equals to one and then generated a kernel by using that window. After that, a convolutional filter is applied to the fused segmented image than by applying re-thresholding and finally, a smoothed image is achieved. Thereafter, holes were filled if there exists any hole.

Figure 4 shows the outputs from JSEG and the RBAC. In the row (a) present, the input images for RBAC segmentation enhanced image is taken as an input. For JSEG segmentation no need for image enhancement and the row (b) shows the binary mask images for both segmentation techniques, the row (c) present the segmented image results after performing the JSEG and RBAC segmentation technique, and the last row (d) shows that the output of fused technique is closer to the output of RBAC, but all those points which are the part of

skin lesion and missed by RBAC are picked from JSEG and the final output image is containing both points.

Evaluation of proposed segmentation technique

The proposed fused segmentation technique is applied to the 900 images presented at "ISIC 2017_Part1_Training_Data" and then created selected only those images whose accuracy was greater than 80%. As in Table 1, it is clearly seen that proposed segmentation method accuracy is higher than the Region based active contour and J-segmentation. Individually, the one technique gave better accuracy in the image but the second technique did not give good accuracy in the same image. As the reference, the image "ISIC_0000145" the accuracy on Region based active contour is 98.2% but on the same image, the accuracy of J-segmentation technique is 88.7%. After applied our proposed fused technique on this image the accuracy is 99.2% which is higher than individual two of these techniques. The average accuracy reported on 15 images by our approach is 95.3% (Table 2).

To evaluate the performance of our proposed fused segmentation technique, we also test it by the 200 images of PH² dataset and here again only those images are selected whose accuracy was more than 80%. By manipulative the accuracy parameter, we can conclude that the discussed proposed fused technique reported the best accuracy instead of using segmentation techniques individually as shown in Table 3. The average accuracy reported on 15 images by our approach is 91.7%.

The resulted segmented image is compared with the ground truth segmented images. As shown in Figure 5, the first row has the input images for segmentation, after that the contrast stretched images, then the segmented binary images, the mapped segmented images, and in the last row the comparison between the ground truth images and segmented image is clearly highlighted using blue contour

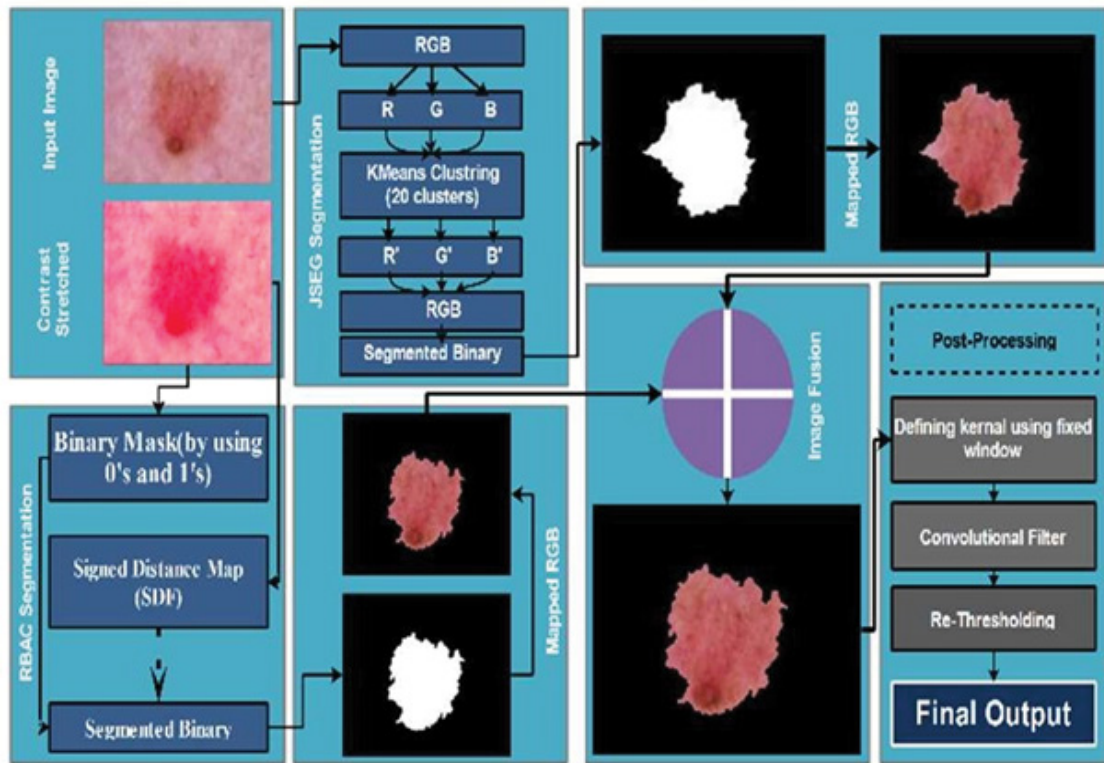


Figure 3. Region-based active contour JSEG fusion technique.

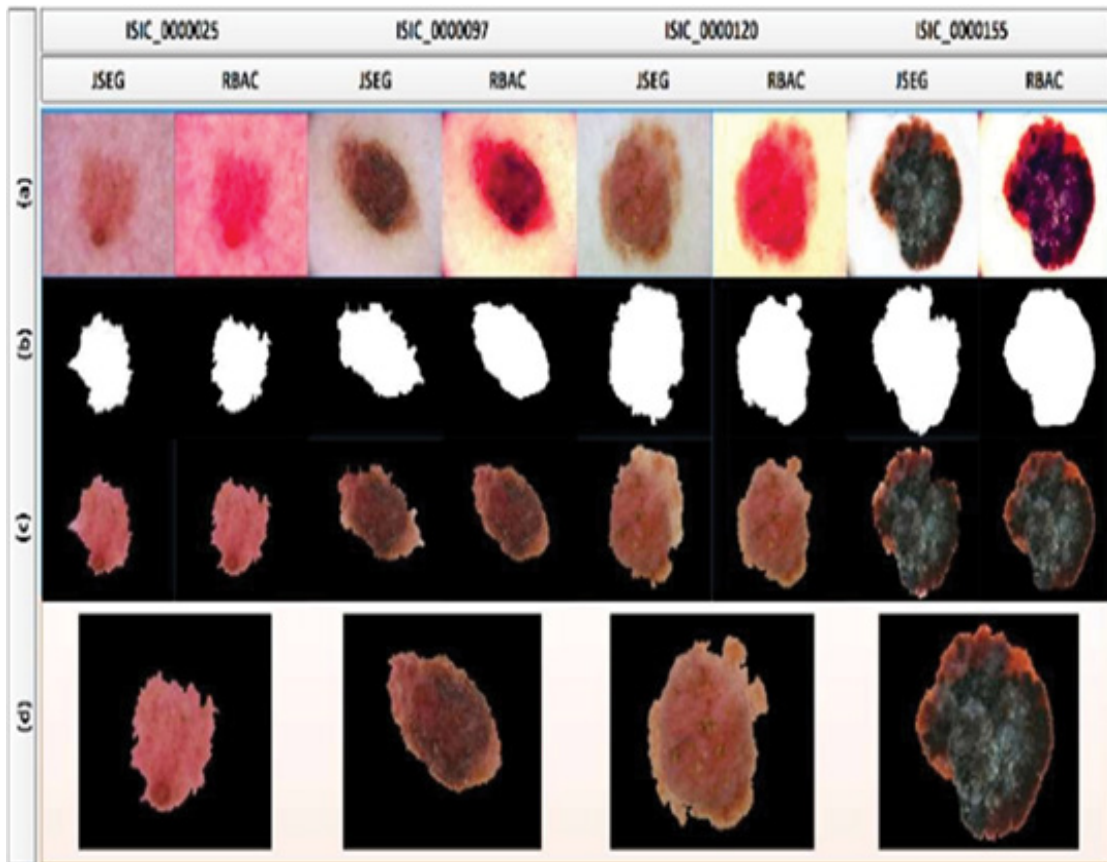


Figure 4. Proposed Segmentation Results, (a) Input Image, (b) Segmented Binary Image, (c) Segmented Mapped RGB image, (d) Fused Image.

representing the segmented image and green representing ground truth contour.

Feature extraction and fusion based on feature selection

For the representation of an image, features play an

Table 1. Proposed segmentation accuracy on dataset ISIC 2017.

Sr No	ISIC 2017 Dataset	Accuracy (%)		
	Image Name	RBAC	JSEG	Proposed Method
1	ISIC_0000145	98.2	88.7	99.2
2	ISIC_0000543	97.6	93.6	98.2
3	ISIC_0000185	96.2	91.6	97.1
5	ISIC_0000104	95.1	95.7	96.3
6	ISIC_0011135	94.9	90.7	95.1
8	ISIC_0000039	93.8	92.2	94.1
9	ISIC_0000093	91.2	95.8	95.9
10	ISIC_0000073	93.6	93.1	94.1
11	ISIC_0000080	93	91.9	93.6
12	ISIC_0010233	92.7	95.4	96
13	ISIC_0010442	92.7	92.1	93.2
14	ISIC_0000016	91.7	92.6	93.2
15	ISIC_0000121	90.9	96.4	97.3
Average		93.9	92.9	95.3

Table 2. Proposed segmentation method performance measures results.

Sr. No	ISIC 2017 Dataset	Performance Measures (%)		
	Image Name	Accuracy	Recall	F-Measure
1	ISIC_0010447	99.2	0.99	0.99
2	ISIC_0000097	96.7	0.97	0.98
3	ISIC_0000001	96.4	0.99	0.98
4	ISIC_0000153	95.7	0.99	0.97
5	ISIC_0010330	95.6	0.96	0.97
6	ISIC_0000531	95.3	0.96	0.97
7	ISIC_0000121	97.3	0.97	0.97
8	ISIC_0000025	94.7	0.95	0.97
9	ISIC_0000505	94.2	0.95	0.97
10	ISIC_0000093	95.9	0.94	0.97
11	ISIC_0000152	93.9	0.93	0.96
12	ISIC_0000465	93.8	0.99	0.96
13	ISIC_0000182	93.2	0.93	0.96
14	ISIC_0000544	92.8	0.92	0.96
15	ISIC_0011135	95.1	0.92	0.96
16	ISIC_0011332	92.7	0.92	0.96
17	ISIC_0000256	92.7	0.93	0.96
18	ISIC_0002093	92.4	0.92	0.96
19	ISIC_0009533	92.3	0.92	0.96
20	ISIC_0000041	92.1	0.92	0.95
21	ISIC_0000225	92.1	0.92	0.95
22	ISIC_0000154	91.9	0.92	0.95
23	ISIC_0000261	91.8	0.91	0.95
24	ISIC_0000089	91.4	0.91	0.95
25	ISIC_0009599	91.1	0.91	0.95
26	ISIC_0000137	91	0.91	0.95
27	ISIC_0000541	90.9	0.9	0.95
28	ISIC_0010442	93.2	0.9	0.95
29	ISIC_0000492	90.5	0.9	0.95
30	ISIC_0000094	90.4	0.94	0.94

important part. In this study, the shape, texture and hand-crafted features are extracted from the segmented image. A total of 870 features categories as into three features: shape (840), texture (57), and hand-crafted (21).

In proposed feature vector is fused by serial fusion technique

Table 3. Proposed segmentation accuracy using PH² dataset.

Sr. No	PH ² Dataset	Accuracy (%)		
	Image Name	RBAC	JSEG	Proposed Method
1	IMD021	96.2	92.4	96.4
2	IMD149	93	93.9	93.9
3	IMD020	92.6	94.2	94.6
5	IMD078	90.9	92.7	92.7
6	IMD164	86.3	92	92
7	IMD041	88.2	90.1	90.2
8	IMD168	86.6	91.5	91.6
9	IMD155	85.2	85.5	85.5
10	IMD169	88.3	87.9	88
11	IMD015	94.4	86.8	94.8
12	IMD016	95.6	88.9	95
13	IMD018	91.6	90	92
14	IMD002	85.5	82.5	85.5
Average		90.30%	89.90%	91.7

as presented in Figure 6. For better features selection entropy based selection is applied on the final feature vector and get the total 800 feature vector. This optimized feature vector will be further helpful in classifying of the lesion into benign or melanoma (Table 4).

Experimental Results

In this article, two benchmark datasets ISIC 2017 and PH² are selected for the assessment of the proposed technique. Both datasets having different dimension RGB dermoscopic skin lesion images. The final results are carry out using FG-SVM (Fine Gaussian) and compared its performance with other classifiers like naive Bayes, Complex Tree (CT), W-KNN, linear discriminant analysis (LDA), Ensemble Boosted Tree (EBT), Ensemble Subspace Discriminant Analysis (ESDA), Linear Regression (LR). After the analysis of these classifiers, only three classifiers are selected for comparison which has the best accuracy. In which cubic-SVM, F-KNN, and ensemble bagged trees are included. The seven statistical measures are calculated including execution time, precision, sensitivity, specificity, false negative rate (FNR), the area under the curve (AUC), and accuracy.

ISIC 2017 Dataset

ISIC (International Skin Imaging Collaboration) contains two types of image data clinical (100 images) and dermoscopic contact non-polarized (2117 images). The training dataset provided by ISIC 2017 dataset contains 2 classes: benign (non-melanoma) which have two sub-classes: nevus and seborrheic keratosis, and melanoma dermoscopic images. As shown in Table 5, the total amount of training images is 2000 in which seborrheic keratosis (254), and benign nevi (1372) the total 1,624 are benign images, and 374 are melanoma images. For testing,

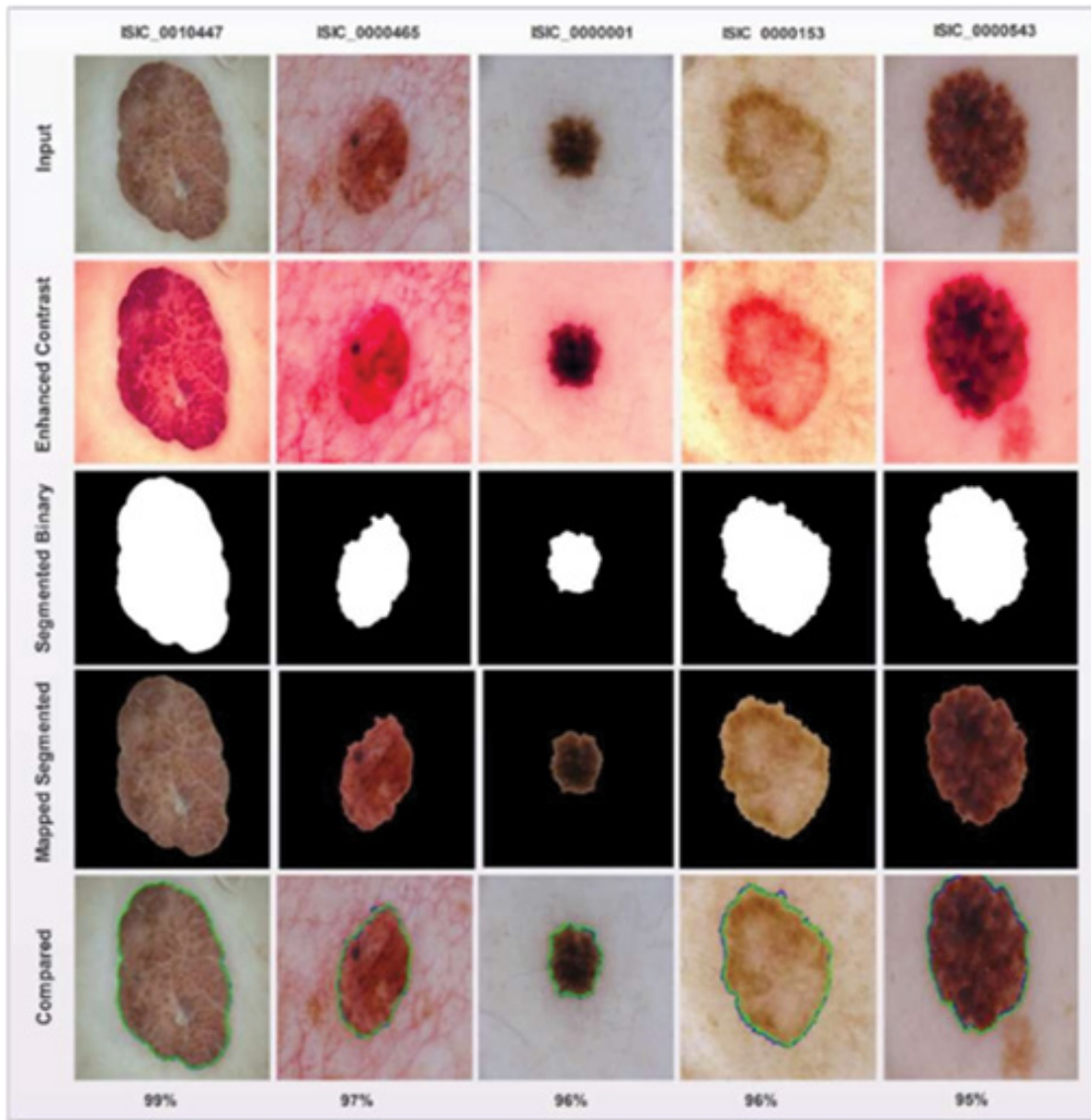


Figure 5. Proposed segmentation steps and comparison of the proposed segmentation method (blue contour) with ground truth area (green contour).

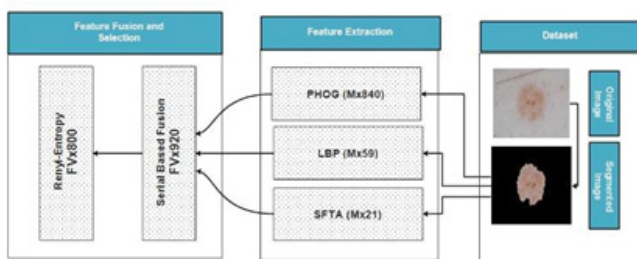


Figure 6. The proposed hybrid feature vector.

there are 600 images in which benign(non-melanoma) are 483 and melanoma are 117 dermoscopic images. In the literature, mostly researcher used publically available ISIC datasets [25-27]. They have been frequently utilized to train and test the model and evaluate the skin lesion segmentation and classification proposes methods.

The 70% data for training and 30% for testing is taken for the evaluation of the proposed method. For every classifier evaluation, the 10-fold cross validation is applied. The proposed method achieved the highest accuracy on FG-SVM

Table 4. Proposed segmentation method performance measures results.

Sr. No	PH ² Dataset	Performance Measures		
	Image Name	Accuracy (%)	Recall (%)	F-Measure (%)
1	IMD021	96.4	0.97	0.98
2	IMD016	95.6	0.98	0.97
3	IMD015	94.4	0.97	0.97
4	IMD149	93	0.93	0.96
5	IMD020	92.6	0.93	0.96
6	IMD018	91.6	0.91	0.95
7	IMD010	91.5	0.98	0.95
8	IMD027	91.3	0.95	0.95
9	IMD038	91.2	0.93	0.95
10	IMD078	90.9	0.91	0.95

which is 99.7%, specificity 1.00%, and sensitivity 99.0% as presented in Table 6.

PH² Dataset

The dermoscopic images were obtained at the Dermatology Service of Hospital Pedro Hispano (Matosinhos, Portugal) under the same conditions through Tuebinger Mole Analyzer system using a magnification of 20x. The PH² database contains a total of 200 dermoscopic images of non-melanoma 160 and 40 melanoma, as shown in Table 7. The PH² database includes medical annotation of all the images namely medical segmentation of the lesion, clinical and histological diagnosis and the assessment of several dermoscopic criteria (colors, pigment network, dots/globules, streaks, regression areas,

blue-whitish veil). The benchmark PH² dataset contains a very small amount of dermoscopic images but the researchers also utilized this dataset for testing or training and evaluation of out efficiently and classifier also classifies into accurate classes [28-30]. A preprocessing step in which their proposed methods. The data augmentation is applied on the class having less no of images, such as Melanoma PH² has the minimum number of images among all classes so data augmentation technique is used on it to balance the classes.

The evaluation of the proposed method on PH² gave the best accuracy on ensemble bagged trees classifier 98.5%

Table 6. Classification results on shape, lbp, texture, and proposed feature vector.

ISIC 2017 Classifiers	Number of Features				Performance Measures (%)						
	Shape	LBP	Texture	Proposed	Time	Precision	Sen.	Spec.	AUC	FNR	Accuracy
	✓				32.28	99	99	1	1	0.3	99.7
FG-SVM		✓			4.39	99	99	0.99	1	0.5	99.5
			✓		3.77	98	98	0.98	1	1.8	98.2
				✓	29.66	99	99	1	1	0.2	99.8
	✓				13.47	97	96.5	0.97	0.99	3.1	96.9
Cubic-SVM		✓			5.67	93.5	92.5	0.92	0.96	7.3	92.7
			✓		14.7	89.5	88.5	0.88	0.92	11.6	88.4
				✓	18.19	97	97	0.97	0.99	2.9	97.1
	✓				10.5	95.5	95	0.95	0.95	4.8	95.2
Fine-KNN		✓			0.66	94	93.5	0.93	0.93	6.6	93.4
			✓		0.61	94.5	93.5	0.94	0.94	6	94
				✓	11.07	95.5	95.5	0.95	0.96	4.5	95.5
	✓				21.82	99	99	0.99	1	0.7	99.3
Ensemble		✓			7.83	98	98	0.98	1	1.7	98.3
Bagged Trees			✓		7.44	97	96.5	0.97	1	3	97
				✓	24.54	99	99	0.99	1	0.5	99.5

Table 7. PH² dataset classes and diagnostic attributes of dermoscopic images.

Classes	Diagnostic Attributes	Total Images (2000)
1	Benign	160
2	Melanoma	40

Table 8. Classification performance measures results on shape, lbp, texture, and proposed feature vector using PH₂.

PH ² Dataset Classifiers	Number of Features				Performance Measures (%)						
	Shape	LBP	Texture	Proposed	Time	Precision	Sen.	Spec.	AUC	FNR	Accuracy
	✓				2.47	92	92.6	0.92	0.98	6.3	93.7
FG-SVM		✓			0.89	96.3	91	0.96	1	3.9	96.1
			✓		0.63	97.6	97.6	0.97	1	2.4	97.6
				✓	3.12	98	98	0.98	1	2	98
	✓				3.1	96.3	96.3	0.96	0.97	3.6	96.4
Cubic-SVM		✓			0.99	93.6	93.6	0.96	0.96	6.6	93.4
			✓		0.68	92.3	92	0.92	0.97	7.8	92.2
				✓	3.07	96.6	96.3	0.96	0.99	3.6	96.4
	✓				1.76	95	95.3	0.95	1	4.8	95.2
Fine-KNN		✓			0.33	96.6	96.3	0.96	0.97	3.6	96.4
			✓		0.29	98	97.3	0.97	0.98	2.7	97.3
				✓	1.88	97.4	97	0.97	0.97	2.3	97.7
	✓				6.67	96.6	97.3	0.97	0.99	2.4	97.6
Ensemble		✓			7.45	96.3	96.3	0.96	1	3.6	96.4
Bagged Trees			✓		3.51	96	96	0.96	0.99	3.9	96.1
				✓	13.82	98.3	98.3	0.98	0.99	1.5	98.5

Table 9. Comparison of our proposed segmentation method with state-of-art baselines.

Benchmark Datasets				
Method	PH ²	ISIC 2017	ISBI 2016	Accuracy (%)
A. Pennisi .et al. [38]	√	-	-	89.6
H. Wen et al. [39]	-	-	√	92.9
Y. Yuan et al. [13]	-	√	-	93
T. Akram et al. [40]	√	-	√	93.2
Proposed Method	√	√	-	95.3

which is higher than as compared to FG-SVM and other classifiers which can see in Table 8.

Discussion

Automatic segmentation of skin lesion from dermoscopic images remains a tricky issue caused by the irregular border, tremendous variation in shape, color and texture of lesions as well as the existence of a range of artifacts such as ruler marks, air bubbles, etc. [29]. The accurate segmentation is necessary to step for acquiring more specific and prominent features, besides for accurate classification. Basically, the performance of all other phases is below of segmentation directly depends on segmentation phases. If segmentation performs accurately than feature selection/extraction carries removal of unnecessary hairs, enhancement of color, is executed plays an essential role in the accurate segmentation of skin lesion. There are many advantages of region-based active contour methods in contrast to edge-based methods. In region-based methods, the statistical detail is used to control the progress of inside and outside of the contour. Also, it gave a good performance in case low or not edges images [31]. One of the more region-based methods is JSEG, used after some modifications and get promising results [32,33].

Recently, in 2017 Codella NC proposed a system for the segmentation and classification of melanoma from dermoscopic images of the skin by using deep learning [34]. The method was evaluated on the largest public benchmark for melanoma recognition available and gets a higher accuracy of 75%. Again in 2017, Sathesha et al. [35] proposed a 3D reconstruction technique for classification of *in situ* (Stage 0) melanoma that incorporates the depth estimation by using 2D dermoscopic images. For segmentation, they used adaptive snake technique. The depth map is estimated to the underlying 2D surface for the achievement of 3D reconstruction. The PH², ISIC: Melanoma Project and ATLAS dermoscopy data sets are considered for experimental evaluations. Their system achieved the sensitivity of 96%, specificity 97% on the PH² dataset and sensitivity 98%, specificity 99% on the ATLAS dataset.

The authors Guo et al. proposed two fully convolutional residual networks (FCRN) for segmentation task [36]. The evaluated their method on the ISIC 2017 dataset and segmentation task achieved 75% accuracy which is not satisfactory performance described an adaptive region growing method for skin lesion segmentation on

dataset ISIC 2017 but their proposed method needs more improvement for accurate segmentation [37-40]. The active contour method (ACM) also known as snakes, used to identify the boundaries of an object by specifying curves on the images. The main problem with the active contour method it cannot works well on sharp edges so different pre-processing steps also performed like Gaussian smoothing, contour construction, and greedy methods. ACM are classified into two groups: edge-based and region based methods. Active contour method is used the curve method for segmentation like active snake algorithm etc. [23]. According to the results, as already discussed above and shown in Table 9, our proposed methodology gain best results as compared to previous methods for skin lesion segmentation.

Conclusion

In this study, we used a joint design that fuses both the RBAC and JSEG method for skin lesion segmentation. Our design technique improved the lesion segmentation as well as deal with the failure cases. The outcomes exhibited an incredible potential by beating state-of-art strategies for skin lesion segmentation from dermoscopic images. The proposed method also deals with different artifact present in the dermoscopic images. In the next study, a novel approach will be proposed for low contrast images by using histogram decision.

Acknowledgment

This work was supported by Artificial Intelligence and Data Analytics (AIDA) Lab Prince Sultan University Riyadh Saudi Arabia. Authors are thankful for the support. The authors are also grateful for the support of the Department of Computer Science, Lahore College for Women University, Jail Road, Lahore 54000, Pakistan.

References

1. Orthaber K, Pristovnik M, Skok K, Perić B, Maver U. Skin cancer and its treatment: novel treatment approaches with emphasis on nanotechnology. *J Nanomater* 2017; 2017.
2. Siegel RL, Miller KD, Jemal A. Cancer statistics, 2018, CA. *Cancer J Clin* 2018; 68: 7-30.
3. Pehamberger H, Steiner A, Wolff K. *In vivo* epiluminescence microscopy of pigmented skin lesions. I . Pattern analysis of pigmented skin lesions. *J Am Acad Dermatol* 1987; 17: 571-583.
4. House D, Moore GE, Roadmap IT. *Moores law viewpoint* 2015.
5. Patel VL, Shortliffè EH, Stefanelli M, Szolovits P, Berthold MR, Bellazzi R, Abu-Hanna A. The coming of age of artificial intelligence in medicine. *Artif Intell* 2009; 46: 5-17.
6. Jiang F, Jiang Y, Zhi H, Dong Y, Li H, Ma S, Wang Y, Dong Q, Shen H, Wang Y. Artificial intelligence in healthcare: Past, present and future. *Stroke Vasc Neurol* 2017; 2: 230-243.
7. Dilsizian SE, Siegel EL. Artificial intelligence in medicine and cardiac imaging: Harnessing big data and advanced computing to provide personalized medical diagnosis and treatment. *Curr Cardiol Rep* 2014; 16: 441.
8. Jha S, Topol EJ. Adapting to artificial intelligence: Radiologists

- and pathologists as information specialists. *J Am Med Assoc* 2016; 316: 2353-2354.
9. Stanley RJ, Stoecker WV, Moss RH. NIH Public Access 2013; 6: 62-72.
 10. Iyatomi H, Oka H, Celebi ME, Hashimoto M, Hagiwara M, Tanaka M, Ogawa K. An improved Internet-based melanoma screening system with dermatologist-like tumor area extraction algorithm. *Comput Med Imaging Graph* 2008; 32: 566-579.
 11. Garcia-Garcia A, Orts-Escolano S, Oprea S, Villena-Martinez V, Garcia-Rodriguez J. A Review on Deep Learning Techniques Applied to Semantic Segmentation. *arXiv preprint* 2017; 22.
 12. Goyal M, Yap MH. Multi-class semantic segmentation of skin lesions *via* fully convolutional networks. *Anal Melanoma Detect* 2017; 28: 1-8.
 13. Yuan Y, Lo YC. Improving dermoscopic image segmentation with enhanced convolutional deconvolutional networks. *IEEE J Biomed Heal Informatics* 2017; 25: 519-526.
 14. Yu L, Chen H, Dou Q, Qin J, Heng PA. Automated melanoma recognition in dermoscopy images *via* very deep residual networks. *IEEE Trans Med Imaging* 2017; 36: 994-1004.
 15. Rashid M, Khan MA, Sharif M, Raza M, Sarfraz MM, Afza F. Object detection and classification : a joint selection and fusion strategy of deep convolutional neural network and SIFT point features. *Multimed Tools Appl* 2019; 78: 15751-15777.
 16. Iyatomi H, Oka H, Saito M, Miyake A, Kimoto M, Yamagami J, Kobayashi S, Tanikawa A, Hagiwara M, Ogawa K, Argenziano G. Quantitative assessment of tumour extraction from dermoscopy images and evaluation of computer-based extraction methods for an automatic melanoma diagnostic system. *Melanoma Res* 2006; 16: 183-190.
 17. Zhang K, Zhang L, Song H, Zhou W. Active contours with selective local or global segmentation: A new formulation and level set method. *Image Vis Comput* 2010; 28: 668-676.
 18. Chan TF, Vese LA. Active contours without edges. *IEEE Trans Image Process* 2001; 10: 266-277.
 19. Li C, Kao CY, Gore JC, Ding Z. Minimization of region-scalable fitting energy for image segmentation. *IEEE Trans Image Process* 2009; 17: 1940-1949.
 20. Lee T, Ng V, Gallagher R, Coldman A, McLean D. Dullrazor®: A software approach to hair removal from images. *Comput Biol Med* 1997; 27: 533-543.
 21. Barata C, Celebi M E. A comprehensive review of image enhancement techniques. *IEEE J. Biomed Heal Informatics* 2018 2: 8-13.
 22. Singh SS, Singh NG, Singh TT, Devi HM. Global-Local contrast enhancement. *Int J Comput Appl* 2012; 54: 975-888.
 23. Silveira M, Nascimento JC, Marques JS, Marçal AR, Mendonça T, Yamauchi S, Maeda J, Rozeira J. Comparison of segmentation methods for melanoma diagnosis in dermoscopy images. *IEEE J Sel Top Signal Process* 2009; 3: 35-45.
 24. Lulio LC, Tronco ML, Porto AJ. JSEG-based image segmentation in computer vision for agricultural mobile robot navigation. *Proc. IEEE Int Symp Comput Intell Robot Autom* 2009; 240-245.
 25. Li X, Wu J, Jiang H, Chen EZ, Dong X, Rong R. Skin lesion classification *via* combining deep learning features and clinical criteria representations. *bioRxiv* 2018.
 26. Chatterjee S, Dey D, Munshi S. Optimal selection of features using wavelet fractal descriptors and automatic correlation bias reduction for classifying skin lesions. *Biomed Signal Process Control* 2018; 40: 252-262.
 27. Al-Masni MA, Al-antari MA, Choi MT, Han SM, Kim TS. Skin lesion segmentation in dermoscopy images *via* deep full resolution convolutional networks. *Comput Methods Programs Biomed* 2018; 162: 221-231.
 28. Ruela M, Barata C, Marques JS, Rozeira J. A system for the detection of melanomas in dermoscopy images using shape and symmetry features. *Comput Methods Biomech Biomed Eng Imaging Vis* 2017; 5: 127-137.
 29. Nasir M, Attique Khan M, Sharif M, Lali IU, Saba T, Iqbal T. An improved strategy for skin lesion detection and classification using uniform segmentation and feature selection based approach. *Microsc Res Tech* 2018; 81: 528-543.
 30. Yuan Y, Chao M, Lo YC. Automatic skin lesion segmentation using deep fully convolutional networks with jaccard distance. *IEEE Trans Med Imag* 2017; 36: 1876-1886.
 31. Sumithra R, Suhil M, Guru DS. Segmentation and classification of skin lesions for disease diagnosis. *Procedia Comput Sci* 2015; 45: 76-85.
 32. Olugbara OO, Taiwo TB, Heukelman D. Segmentation of melanoma skin lesion using perceptual color difference saliency with morphological analysis. *Math Probl Eng* 2008; 1-19.
 33. Emre Celebi M, Alp Aslandogan Y, Stoecker WV, Iyatomi H, Oka H, Chen X. Unsupervised border detection in dermoscopy images. *Ski Res Technol* 2007; 13: 454-462.
 34. Codella NC, Nguyen QB, Pankanti S, Gutman DA, Helba B, Halpern AC, Smith JR. Deep learning ensembles for melanoma recognition in dermoscopy images. *Ibm J Res Dev* 2016; 61: 1-28.
 35. Satheesha TY, Satyanarayana D, Prasad MG, Dhruve KD. Melanoma is skin deep: a 3d reconstruction technique for computerized dermoscopic skin lesion classification. *IEEE J Transl Eng Heal Med* 2017; 5: 1-7.
 36. Li Y, Shen L. Skin lesion analysis towards melanoma detection using deep learning network. *Sensors*. 2018; 18: 556.
 37. Guo Y, Ashour A, Smarandache F. A novel skin lesion detection approach using neutrosophic clustering and adaptive region growing in dermoscopy images. *Symmetry* 2018; 10: 119.
 38. Pennisi A, Bloisi DD, Nardi D, Giampetruzzi AR, Mondino C, Facchiano A. Computerized medical imaging and graphics skin lesion image segmentation using delaunay triangulation for melanoma detection. *Comput Med Imaging Graph* 2016; 52: 89-103.
 39. Wen H. II-FCN for skin lesion analysis towards melanoma detection. *arXiv* 2017.
 40. Akram T, Khan MA, Sharif M, Yasmin M. Skin lesion segmentation and recognition using multichannel saliency estimation and M-SVM on selected serially fused features. *J Ambient Intell Humaniz Comput* 2018; 1-20.

***Correspondence to**

Rabia Javed

Department of Engineering

Universiti Teknologi Malaysia

Johor Bahru

Malaysia